Environmental Pollution 270 (2021) 116269

Contents lists available at ScienceDirect

Environmental Pollution

journal homepage: www.elsevier.com/locate/envpol

Enantioselective residues and toxicity effects of the chiral triazole fungicide hexaconazole in earthworms (*Eisenia fetida*)☆

Tong Liu [a, 1], Kuan Fang [a, b, 1], Yalei Liu [a, b], Xiaolian Zhang [a, b], Lingxi Han [b], Xiuguo Wang [a, *]

[a] Tobacco Research Institute of Chinese Academy of Agricultural Sciences (CAAS), Qingdao, 266101, PR China
[b] Graduate School of Chinese Academy of Agricultural Sciences, Beijing, 100081, PR China

ARTICLE INFO

Article history:
Received 12 October 2020
Received in revised form
29 November 2020
Accepted 7 December 2020
Available online 10 December 2020

Keywords:
Hexaconazole
Earthworm
Enantioselectivity
Bioaccumulation
Toxicity

ABSTRACT

The enantioselective toxic effect and environmental behavior of chiral pesticides have attracted increasing research attention. In this study, the enantioselective toxicity and residues of hexaconazole (HEX) in earthworms (*Eisenia fetida*) were investigated. In the present study, significant enantioselective degradation characteristics were observed in artificial soil with the *R*-enantiomer preferentially degrading ($p < 0.05$); however, no significant enantioselective bioaccumulation was observed in the earthworms ($p > 0.05$). The acute toxicity of *S*-(+)-HEX was higher than that of *R*-(−)-HEX in earthworms, with 48-h LC_{50} values of 8.62 and 22.35 μg/cm^2, respectively. At 25 mg/kg, enantiospecific induction of oxidative stress was observed in earthworms; moreover, *S*-(+)-HEX had a greater influence on the contents of malonaldehyde, cytochrome P450, and 8-hydroxy-2-deoxyguanosine than *R*-(−)-HEX. These results were consistent with those of the enrichment analysis of differentially expressed genes. The transcriptome sequencing results showed that *S*-(+)-HEX had a more significant influence on steroid biosynthesis, arachidonic acid metabolism, and cell cycle processes than *R*-(−)-HEX, leading to abnormal biological function activities. These results indicate that *S*-(+)-HEX may pose a higher risk to soil organisms than *R*-(−)-HEX. This study suggests that the environmental risk of chiral pesticides to nontarget organisms should be assessed at the enantiomeric level.

Credit author statement

Tong Liu, Conceptualization, Data curation, Writing-reviewing and editing, Project administration, Funding acquisition. Kuan Fang, Data curation, Writing − original draft, preparation, Investigation. Yalei Liu, Investigation. Xiaolian Zhang, Investigation. Lingxi Han, Investigation. Xiuguo Wang, Conceptualization, Supervision, Funding acquisition.

1. Introduction

The nature of a substance to be unable to overlap with its mirror image is called chirality (Gao et al., 2020). The importance of molecular chirality in the natural sciences has been increasingly valued since the optical isomers of tartaric acid were separated by Pasteur (Ma et al., 2011). Additionally, the chirality problem has received increased attention in the field of pesticide research. More than 1600 pesticides are being sold on the pesticide market, and 30% of them have the characteristic of chirality (Gao et al., 2020). However, for economic reasons, most are sold in the form of mixtures of enantiomers or racemates, and only 7% are used as a single enantiomer (Garrison, 2011; Gao et al., 2020). Moreover, the enantioselectivity of some pesticides in terms of ecological security is poorly understood (Gámiz et al., 2016). Thus, racemic pesticides may contain ineffective or even harmful enantiomers that not only reduce the efficacy but are also more likely to cause phytotoxicity and resistance (Han et al., 2013). Therefore, to promote green pesticides and sustainable development, it is imperative to study the different effects of enantiomers.

Hexaconazole (HEX) [(RS)-2-(2,4-dichlorophenyl)-1-(1H-1,2,4-triazol-1-yl) hexan-2-ol], which belongs to the class of triazole fungicides, is a sterol demethylation inhibitor with two enantiomers: *R*-(−)-HEX and *S*-(+)-HEX. HEX has broad-spectrum

☆ This paper has been recommended for acceptance by Christian Sonne.
* Corresponding author.
E-mail address: wangxiuguo@caas.cn (X. Wang).
[1] These authors contributed equally: Tong Liu and Kuan Fang.

https://doi.org/10.1016/j.envpol.2020.116269
0269-7491/

eradication effects on fungal diseases, especially those caused by basidiomycetes and ascomycetes, by inhibiting ergosterol synthesis to deter the growth of fungal mycelia (Han et al., 2013). HEX is widely used on vegetables, field crops, and fruits because of its high efficiency, low toxicity, and broad spectrum (Zhang et al., 2012a; Han et al., 2013). Like other triazole compounds, HEX also has plant growth-regulating properties, which can induce many morphological changes such as promoting rooting, inhibiting gibberellin synthesis, and increasing the chlorophyll and ABA contents (Liang et al., 2011; Zhang et al., 2012b). Therefore, HEX is expected to become a widely used fungicide worldwide.

However, a previous study has shown that HEX may pose a potential risk to the environment (Ju et al., 2017). HEX has a long persistence in soil with a half-life of 225 days (Ju et al., 2017). Additionally, the initial residual concentration of HEX in the soil environment is between 0.056 and 2.74 mg/kg (Wang et al., 2012, 2014; Maznah et al., 2015). Moreover, HEX has good water solubility and fluidity and can percolate to the groundwater through the soil after application in the field, which may have adverse effects on mammals including rats (Shen et al., 2013). Additionally, HEX has shown moderate acute toxicity to aquatic invertebrates. Yu et al. (2013) have reported that HEX can induce oxidative stress and the upregulation of target genes in zebrafish. Ju et al. (2017) have found that excessive application of HEX is harmful to soil microorganisms. Therefore, HEX may be a potential soil contaminant, and thus, its threat to the soil environment should be carefully considered. Moreover, some studies have shown that HEX enantiomer exposure leads to enantioselective degradation after application to crops such as tomato, cucumber, and head cabbage (Wang et al., 2012; Li et al., 2013). Notably, no studies have examined the differences in the environmental behavior of HEX enantiomers and their effects on the soil environment. Therefore, it is necessary to assess the environmental safety of HEX in the soil environment at the enantiomeric level.

In this study, the enantioselective residual characteristics of HEX enantiomers in soil and earthworms were investigated based on residual degradation tests and toxicity tests. Moreover, the enantioselective differences induced by *R*-(−)-HEX and *S*-(+)-HEX in acute toxicity and oxidative stress response in earthworms were studied. This study aimed to investigate the environmental safety of HEX at the enantiomeric level and provide a database for the appropriate use of chiral pesticides.

2. Materials and methods

2.1. Materials

R-(−)-HEX (99.0%) and *S*-(+)-HEX (99.0%) were obtained by splitting the HEX racemate. Earthworms (*Eisenia fetida*) were provided by the Qingdao (China) earthworm breeding base. The purchased earthworms were nurtured at 20 ± 2 °C and kept in a mixed substrate containing peat moss and cow dung for two weeks under a 12-h light/dark cycle. Healthy adults (350 ± 20 mg) were selected and placed on moist filter paper for 24 h before the experiment. In this study, the tested soil was artificial soil that met the Organization for Economic Co-operation and Development (OECD) standards and comprised 10% peat moss, 20% kaolin clay, and 70% quartz sand. An appropriate amount of calcium carbonate was added to adjust the pH of the artificial soil to 6.0 ± 0.5.

2.2. Acute toxicity test

The filter paper contact test was conducted following the standard of the OECD guideline 207 (OECD, 1984). A filter paper of reasonable size was placed into an uncovered glass tube (8 cm in length, 3 cm in diameter). The filter paper method was set using experimental concentrations of 66.40, 53.12, 39.84, 26.56, 19.92, 13.28, 6.64, 3.32, and 1.66 μg/cm^2. *R*-(−)-HEX and *S*-(+)-HEX were dissolved in methanol and loaded onto the filter paper (1 mL solution per glass tube). Control groups were also run in parallel, with 1.0 mL of methanol only. After the methanol was evaporated in a fume hood, the filter paper was rewetted with 1 mL of distilled water. One earthworm treated at the bowel was placed in each glass tube, which was then sealed with a porous parafilm and maintained in the dark at 20 ± 1 °C. Earthworm mortality was calculated at 24 and 48 h. The criterion for judging earthworm death was no response in the head or tail with slight irritation. Fifteen parallels were set for each experimental concentration.

2.3. Sub-chronic toxicity test

In previous studies, the initial residual concentrations of HEX in the soil environment ranged from 0.056 to 2.74 mg/kg (Wang et al., 2012, 2014; Maznah et al., 2015). Generally, environmental workers often choose 5–10 times the initial residual concentrations of target compounds as the concentration for sub-chronic toxicity tests (Ma et al., 2019; Wang et al., 2020; Zhang et al., 2012b). Additionally, according to the study by Chen et al. (2013), an obvious bioaccumulation phenomenon was observed when the earthworms were exposed to the racemic HEX at a concentration of 25 mg/kg (dry weight) for the sub-chronic toxicity test. Therefore, to maximize the risk assessment, the exposure concentration was close to 10 times that of the maximum initial residue, that is, 25 mg/kg. Approximately 750 g of artificial soil that was thoroughly mixed with the desired amount of pesticide solution was added to a 1 L glass beaker, and the artificial soil moisture was adjusted to 35% with deionized water. Twenty-five earthworms were placed into each glass beaker that was covered with a porous parafilm to allow aeration. Each treatment was prepared for five beakers. The earthworms were nurtured at 20 ± 2 °C with a 12-h/12-h light-dark regime. The control groups were prepared similarly but without target compound application. At 3, 7, 14, 28, and 42 days after exposure, the earthworm and soil samples were randomly collected for different analyses. Before measuring each indicator, the earthworms were washed with deionized water and placed on wet filter paper for 24 h to remove their intestinal contents.

2.4. Enantioselective residues of HEX enantiomers in earthworms and artificial soil

Soil and earthworm sample treatments. The earthworms and artificial soil samples were sampled at 3, 7, 14, 28, and 42 days after exposure. Five grams of artificial soil was added to a 50 mL centrifuge tube, to which 5 mL of deionized water was added, followed by shaking the mixture to wet the sample. After letting it stand for 10 min, 25 mL of acetonitrile was added to the 50 mL centrifuge tube. For the earthworm samples, three gut-cleansed earthworms were collected and homogenized with deionized water (w/v, 1:2). Next, to extract the compounds from the earthworms, acetonitrile (w/v, 1:5) was added. Then, the earthworms and soil samples were shaken for 5 min on a vortex mixing shaker, and 0.5 g of NaCl and 2 g of $MgSO_4$ were added, followed by shaking for 5 min and centrifugation at 4000 rpm for 5 min. Subsequently, 1.5 mL of the supernatant was placed in a centrifuge tube containing 50 mg of primary secondary amine (PSA). After shaking the contents for 5 min, the sample was centrifuged at 10,000 rpm for 5 min. Thereafter, the collected supernatant was passed through a 0.22 μm filter prior to detection analysis.

2.5. Ultra-performance liquid chromatography–tandem mass spectrometry analysis

The contents of *R*-(−)-HEX and *S*-(+)-HEX were chromatographically detected using an ultra-performance liquid chromatography system coupled with a mass spectrometry system (TSQ Endura, Thermo Fisher Scientific Inc., San José, CA, USA). The liquid chromatography column was a Thermo Hypersil GOLD C_{18} column (2.1 mm × 100 mm, 1.9 μm). The source parameters were a capillary voltage of 3000 V and a capillary temperature of 350 °C. The flow rate was 0.25 mL/min. The injection volume was 2 μL. The mobile phase of acetonitrile (A) and 0.1% formic acid water (B) were used to separate the target compounds, and the mobile phase gradient started at 10% A (0–0.5 min), increased to 90% A (1–4 min), and then decreased to 10% A (4.1–5 min). Multiple reaction monitoring (MRM) mode and positive electrospray ionization (ESI^+) were used to detect the HEX enantiomers. The qualitative and quantitative ion pairs were 314/159 (m/z) and 314/70 (m/z), respectively, when the collision energy was set to 29 eV and 20 eV, respectively.

Based on the conventional validation procedure, the following data were tested to evaluate the performance of the developed method: linearity, precision, accuracy, limits of detection (LODs), and the limits of quantification (LOQs). Evaluation of the HEX enantiomer linearity was performed by adding the two enantiomers to the earthworm and soil matrix extraction solution at different levels (0.001, 0.005, 0.010, 0.050, 0.10, 0.50, 1.0, and 5.0 mg/kg). The accuracy and precision of the developed method were determined by recovery assays, which contained five replicates of the soil and earthworm matrices at three different concentrations (0.010, 0.10, and 25 mg/kg). The LODs of the four target compounds were defined as the concentration that produced a signal-to-noise (S/N) ratio of 3, and the LOQs were considered to be the concentration yielding an S/N ratio of 10.

2.6. Measurement of the oxidative stress effect

One earthworm from each beaker was added to an abrader after it was randomly selected and weighed. Next, the earthworms were homogenized in 50 mM phosphate buffer (pH 7.8) at a dilution of 1/10 (w/v). Subsequently, the homogenized tissue was centrifuged at 8000 ×*g* for 10 min. All samples throughout the process were treated with an ice bath. The method described by Bates et al. (1973) was followed to determine the protein content, and Coomassie brilliant blue was used as the color reagent.

Acetylcholinesterase (AChE), catalase (CAT), and superoxide dismutase (SOD) activities as well as malondialdehyde (MDA) content were determined according to the method described by Zhang et al. (2019a) using a kit obtained from Suzhou Comin Biotechnology Co., Ltd. (Suzhou, China). The respective determination of AChE, CAT, and SOD activities as well as the MDA content were measured using a spectrophotometer and calculated from the respective standard curve.

The hydroxyl radical ($\cdot OH^-$) content, 8-hydroxy-2-deoxyguanosine (8-OHdG) content, and cytochrome P450 (CYP450) activity were determined according to the method described by Zhang et al. (2020) using a kit obtained from the Shanghai HengYuan Biological Technology Co., Ltd. (Shanghai, China). The respective contents were determined according to the instructions of the 8-OHdG, $\cdot OH^-$, and CYP450 ELLSA kits; the absorbance (OD value) was measured using a microplate reader at a wavelength of 450 nm; and the 8-OHdG, $\cdot OH^-$, and CYP450 concentrations in the sample were calculated from the standard curve.

2.7. Transcriptomic analysis

Three gut-cleansed earthworms in each treatment were collected randomly for analysis on day 42. The RNApure plant kit (Aidlab, China) was used to isolate total RNA from each treatment. A NanoPhotometer spectrophotometer (Thermo Fisher Scientific, USA) and an Agilent 2100 bioanalyzer (Agilent, USA) were used to test the purity and integrity of the RNA, respectively. Oligo (dT) magnetic beads were used to enrich mRNA from total RNA. Subsequently, the mRNA was fragmented in NEB fragmentation buffer. The cDNAs were synthesized by the RNA fragments using random hexamers, and then, end repair was used to synthesize, purify, and modify the cDNAs to construct a library. The library was sequenced using the Illumina HiSeq 4000 platform (Illumina, Inc., San Diego, CA, USA). Next, the reads were processed and analyzed using Trinity software. A p-value < 0.01 and |log2 (foldchange)| > 2 was set as the threshold for significant differential expression. Subsequently, the differential expression of functional genes was annotated using the KEGG database.

2.8. Statistical analysis

The first-order kinetic equation was used to simulate the degradation behavior of HEX enantiomers in artificial soil. The degradation equation and half-life ($T_{1/2}$) were calculated using equations (1) and (2):

$$C_t = C_0 e^{-kt} \quad (1)$$

$$T_{1/2} = \ln 2 \Big/ k \quad (2)$$

where C_t represents the concentration (mg/kg) of the test compounds at time t (day) in artificial soil, C_0 represents the initial concentration (mg/kg), and k represents the dissipation rate constant.

$$BSAF = C_E / C_S \quad (3)$$

In the present study, the bioaccumulation of HEX enantiomers was expressed by the biota to soil accumulation factor (BSAF). C_{EW} and C_S represent the concentrations (mg/kg) of the test compounds in the earthworms and artificial soil, respectively.

All statistical analyses were conducted using SPSS software (Version 19.0; SPSS Inc.), and all data were expressed as the mean ± standard deviation (mean ± SD, n = 3). Origin 8.5 software was used to draw the figures. Analysis of variance (ANOVA) with the LSD test was used to analyze the significance ($p < 0.05$) of the data obtained from the indicators.

3. Results and discussion

3.1. Enantioselective residues of HEX enantiomers in soil and earthworms

As shown in Table S1, this method showed excellent linearity ($R^2 \geq 0.9968$) and satisfactory recoveries (93%–108%) at the three spiked levels of 0.010, 0.10, and 25 mg/kg with the relative standard deviation (RSD) values lower than 4.7% in both the soil and earthworm matrices. The LODs of *S*-(+)-HEX in the soil and earthworm matrices were 0.002 mg/kg and 0.003 mg/kg, respectively, whereas the LOQs were 0.007 mg/kg and 0.01 mg/kg, respectively. The LODs of *R*-(−)-HEX in the soil and earthworm matrices were 0.001 mg/kg and 0.002 mg/kg, respectively, whereas the LOQs were 0.004 mg/kg

and 0.006 mg/kg, respectively. The matrix effect values of *S*-(+)-HEX and *R*-(−)-HEX in the soil matrices were 11.2% and 12.1%, respectively, whereas those in the earthworm matrices were −65.3% and −65.7%, respectively. According to the study by Tian et al. (2016), the matrix effect could be ignored when the value ranged from −10% to 10%. In this study, the matrix effect values were not in this range; therefore, the matrix-matched calibration curve was chosen to normalize the matrix effect and obtain more precise results.

The degradation of *R*-(−)-HEX and *S*-(+)-HEX in the artificial soils at a concentration of 25 mg/kg was a time-dependent process (Fig. 1A). As shown in Table S2, the *R*-(−)-HEX and *S*-(+)-HEX degradation corresponded to first-order kinetics, with correlation coefficient (R^2) values of 0.9756 for *R*-(−)-HEX and 0.9345 for *S*-(+)-HEX. The degradation of *R*-(−)-HEX and *S*-(+)-HEX showed different degradation trends during the entire exposure period, with half-lives of 184.8 and 246.4 days, respectively. These results showed that enantioselective degradation occurred between the HEX enantiomers, and the stability of the two target compounds followed the order *S*-(+)-HEX > *R*-(−)-HEX in the soil. The reduction in the content of the two target compounds may be caused by photolysis, earthworm absorption, and microbial decomposition (Liu et al., 2018b). In this study, the bioaccumulation of HEX enantiomers in earthworms showed that the *R*-(−)-HEX and *S*-(+)-HEX content in earthworms increased with the chemical exposure time (Fig. 1B). Moreover, the BSAF value of the *R*-(−)-HEX was smaller than that of *S*-(+)-HEX, suggesting that *S*-(+)-HEX was preferentially accumulated over the *R*-(−)-HEX in earthworm tissue. The present results demonstrated that there was an enantioselective bioaccumulation behavior in the earthworms between *S*-(+)-HEX and *R*-(−)-HEX. Yu et al. (2012) studied the enantioselective bioaccumulation of the triazole fungicide tebuconazole in earthworms, the results of which were similar to our present results. In their study, the *R*-(+)-tebuconazole showed preferential accumulation in earthworm tissue compared with *S*-(−)-tebuconazole. Additionally, Han et al. (2013) reported the obvious enantioselectivity of HEX enantiomers in tomatoes and found that (−)-HEX degraded faster than (+)-HEX in tomatoes, resulting in the enrichment of (+)-HEX. Thus, previous studies and the present results indicate that the bioaccumulation and degradation behavior in the environment of chiral compound enantiomers may be different.

3.2. Acute toxicity of HEX enantiomers to earthworms

The filter paper contact test results showed that the 48-h LC_{50} values of *S*-(+)-HEX and *R*-(−)-HEX in earthworms were 8.62 and 22.35 μg/cm^2, respectively (Fig. 2). Thus, the acute toxicity of *S*-(+)-HEX was stronger than that of *R*-(−)-HEX. Previous studies have investigated the enantioselective toxicity induced by HEX enantiomers; however, a different result was found in the report by Han et al. (2013), who demonstrated that *R*-(−)-HEX showed 11–13-fold higher acute toxicity to four target fungi based on the 48-h LC_{50} value. Furthermore, other chiral fungicides such as benalaxyl, tebuconazole, and metalaxyl also show marked enantioselective differences in acute toxicity to earthworms (Xu et al., 2009; Yu et al., 2012; Zhang and Zhou, 2019b). Chiral compounds undergo a series of biological activities in organisms; therefore, the bio-uptake, transport, assimilation, accumulation, and metabolism of earthworms may induce enantioselective differences in acute toxicity (Konwick et al., 2006). Until now, little information has been available on the acute toxicity difference between HEX enantiomers in the nontarget organism *E. fetida*. The present study provides a basis for accurately evaluating the environmental risks of HEX.

3.3. Enantioselective behavior and toxicity

The statistical analysis of the degradation half-life in artificial

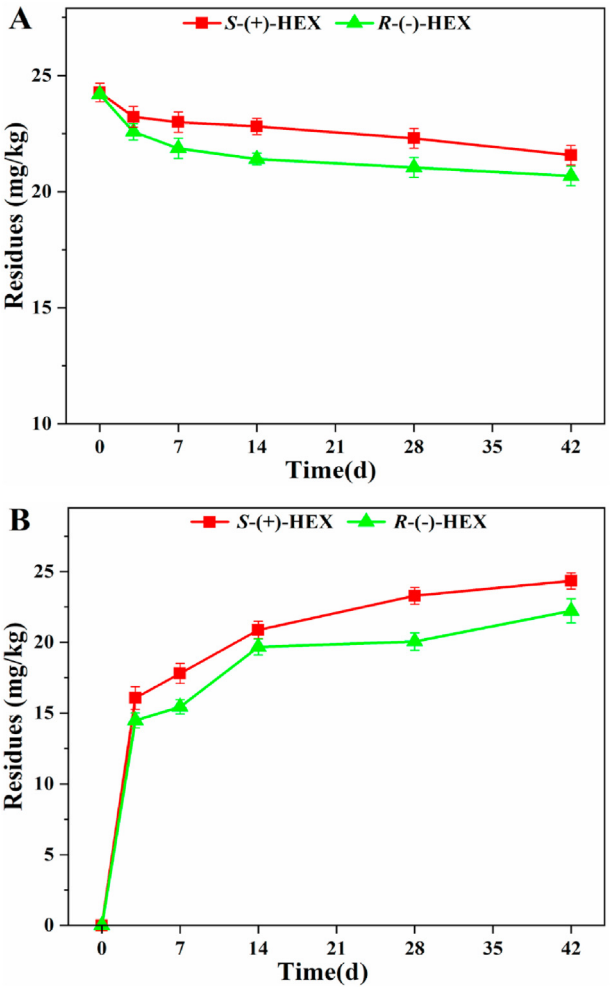

Fig. 1. Residues of *S*-(+)-HEX and *R*-(−)-HEX in the artificial soil (**A**) and earthworms (**B**).

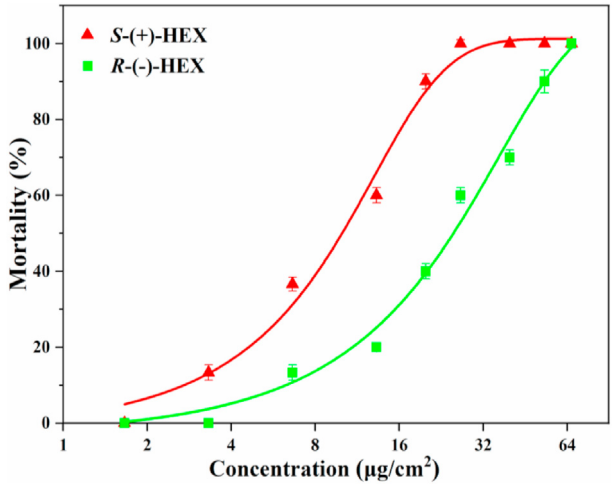

Fig. 2. Dose-effect curves of the for the filter paper contact test of earthworms after exposure to *S*-(+)-HEX and *R*-(−)-HEX. X axis is based on log2.

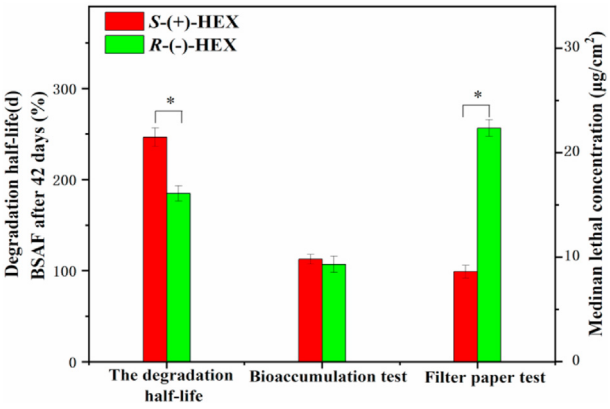

Fig. 3. Statistical analysis of the degradation half-life in artificial soil, bioaccumulation test, and filter paper test (*$p < 0.05$ between treatments).

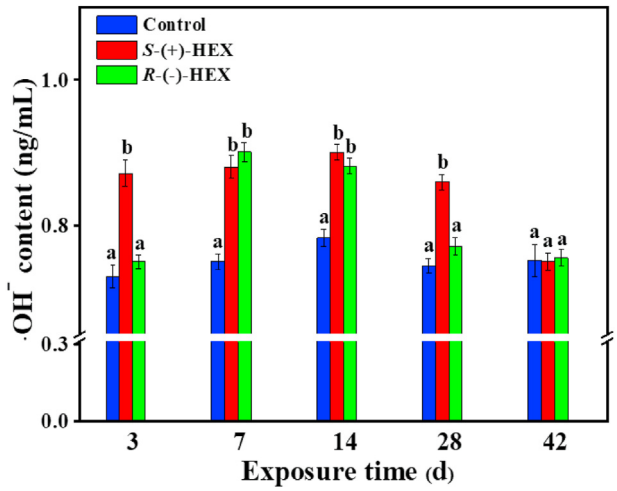

Fig. 4. The ·OH⁻ content changes in earthworms after exposure to *S*-(+)-HEX and *R*-(−)-HEX.

soil, bioaccumulation test, and filter paper test is shown in Fig. 3. Acute toxicity test results showed that significant differences were found in the filter paper experiment ($p < 0.05$). Additionally, compared with the *R*-(−)-HEX treatment, the *S*-(+)-HEX treatment showed 2.59-fold higher acute toxicity to earthworms based on the 48-h LC_{50} value. Notably, Han et al. (2013) studied the enantioselective toxicity of *Daphnia magna* induced by HEX enantiomers, and their study indicated that *R*-(−)-HEX may have higher toxicity to aquatic species. In the present study, significant differences were observed in the degradation half-life of *S*-(+)-HEX and *R*-(−)-HEX ($p < 0.05$). This result demonstrated that enantioselective degradation behavior was observed, and a similar degradation behavior of the triazole fungicide tebuconazole has been reported by Cui et al. (2018). In their study, *S*-(+)-tebuconazole showed preferential degradation in different soils. However, in the present study, no significant differences were found in the bioaccumulation test, although the BSAF value of the *R*-(−)-HEX was smaller than that of the *S*-(+)-HEX ($p > 0.05$). Interestingly, Liu et al. (2014) reported that the enantioselective accumulation of triadimefon enantiomers was not found in soil, whereas the preferential accumulation of *S*-triadimefon was observed in tubifex worms (*Tubifex tubifex*). Hence, the different chiral environments may be of great significance to the enantioselective bioaccumulation behaviors. In general, the acute toxicity and degradation behavior of HEX enantiomers with respect to earthworms in artificial soil were significantly enantioselective, but there was no significant difference in its bioaccumulation behaviors.

3.4. Effects of S-(+)-HEX and R-(−)-HEX on the ·OH⁻ activity in earthworms

It is now widely believed that reactive oxygen species (ROS) production and/or the inhibition of systems that counteract them at least partly cause the negative effects of various environmental stresses (Dubey et al., 2015). The ROS generated by external stimuli including hydrogen peroxide (H_2O_2), hydroxyl radicals (·OH^-), and superoxide anion free radicals ($O_2{\cdot}^-$) have been shown to be related to the occurrence of cell carcinogenesis, aging, and apoptosis (Feng et al., 2017). Among them, ·OH^- is considered the most active and hazardous free radical that is critical in mediating oxygen toxicity *in vivo* (Zhou et al., 2015). Additionally, ·OH^- has been demonstrated to be produced from the chemical reaction between H_2O_2 and $O_2{\cdot}^-$ and external stress conditions (Gill et al., 2010). In the present study, the ·OH^- levels were significantly enhanced after exposure to *S*-(+)-HEX on day 3 ($p < 0.05$) (Fig. 4). Compared with the control treatments, the ·OH^- activity in both *S*-(+)-HEX and *R*-(−)-HEX treatments showed a significant increase on days 7 and 14 ($p < 0.05$). However, the *R*-(−)-HEX treatment returned the ·OH^- activity to control levels on day 28. No significant difference was observed between the treatment and control groups on day 42 ($p > 0.05$). This result indicated that the oxidative stress effects were induced in the earthworms during the early stage of exposure to HEX enantiomers. However, the earthworms gradually overcame the adverse effects induced by the HEX enantiomers, which was probably because the antioxidant defense system of the earthworms was protecting them from damage. Moreover, both *S*-(+)-HEX and *R*-(−)-HEX can cause oxidative stress effects, and the former is stronger. A previous report has demonstrated that HEX can cause oxidative stress effects in the target bacterium *Bradyrhizobium japonicum* (Shahid and Khan, 2018). Additionally, Gao et al. (2013) have reported that the triazole fungicides—triadimenol, difenoconazole, and propiconazole can inhibit the activity of glutathione peroxidase (GSH-Px), which can scavenge the free radicals and lipid peroxide induced by ·OH^- (Gao et al., 2013). Similar to the results of the previous studies, the present study showed that HEX enantiomers could induce abnormal changes in ·OH^- content. Additionally, enantioselective changes in ·OH^- activities were observed in the earthworm bodies after exposure to HEX enantiomers.

3.5. Effects of HEX enantiomers on biological enzyme activities in earthworms

Under external environmental pressure, free radicals such as the peroxide anion and superoxide anion radicals appear in the body and disrupt body functions (Liu et al., 2010). SOD is considered the most effective enzyme with regard to the removal of $O_2{\cdot}^-$ by converting $O_2{\cdot}^-$ to H_2O_2 and O_2, representing the first line of defense against ROS (Liu et al., 2016). As shown in Fig. 5A, compared with the control treatment, SOD activity decreased significantly after exposure to *S*-(+)-HEX and *R*-(−)-HEX on days 3 and 7 ($p < 0.05$). However, no significant difference was observed on day 14 ($p > 0.05$). Additionally, the *S*-(+)-HEX treatments induced a significant increase in SOD on days 28 and 42 ($p < 0.05$). Animal CAT is an enzyme containing heme, which can convert H_2O_2 into water and O_2 (Chen et al., 2016). In the present study, CAT activity decreased significantly following *R*-(−)-HEX and *S*-(+)-HEX exposure on days 3 and 7 compared with the activity observed for the control treatment ($p < 0.05$, Fig. 5B). However, a significant increase

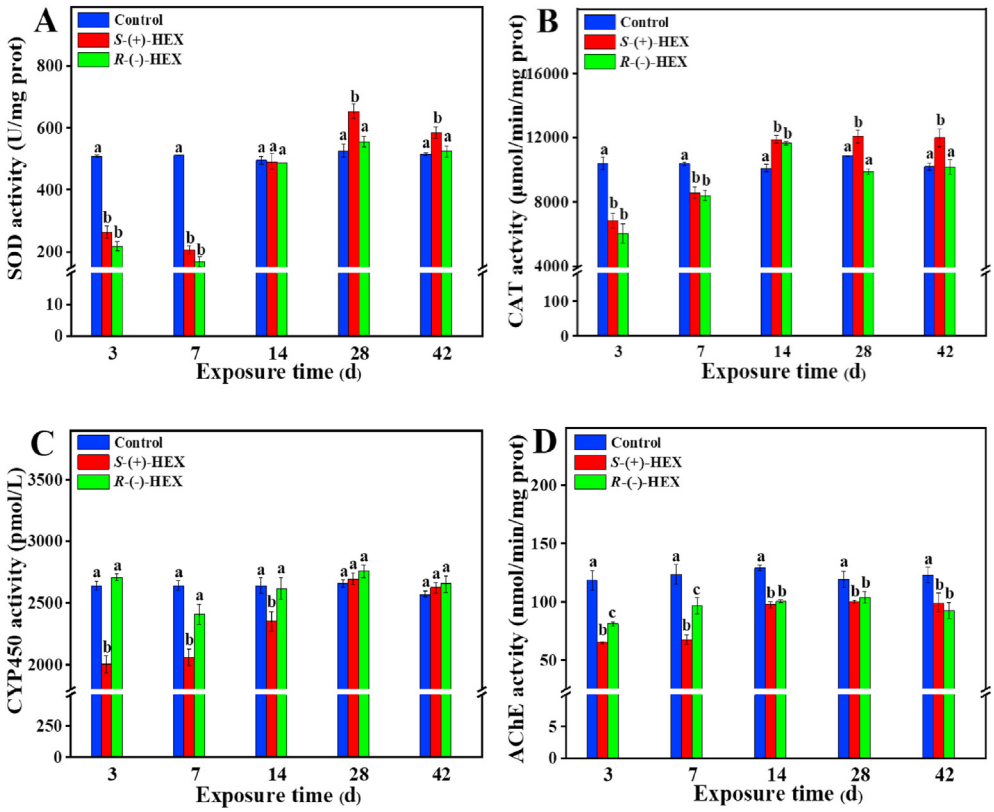

Fig. 5. Effects of *S*-(+)-HEX and *R*-(−)-HEX on SOD activity (**A**), CAT activity (**B**), CYP450 activity (**C**), and AChE activity (**D**) in earthworms.

following the two enantiomer treatments was observed on day 14 ($p < 0.05$). Additionally, the *R*-(−)-HEX treatment resulted in a return to the control levels on days 28 and 42; however, for the *S*-(+)-HEX treatments, a significant increase in CAT activity continued until day 42 ($p < 0.05$). The increase in SOD and CAT enzyme activities was a direct response to the ROS produced by exogenous pollution, whereas the decrease in SOD and CAT enzyme activities might be because the enzymes present were insufficient to clear ROS and because the antioxidant defense system was overwhelmed by a large excess of ROS (Chen et al., 2016). In the present study, SOD and CAT enzyme activity systems were damaged at the beginning of exposure, leading to a decrease in the SOD and CAT contents. After a period of restoration, the SOD and CAT enzyme activity systems worked normally and could respond to stress, leading to an increase in SOD and CAT activities. The altered SOD activity and CAT activity demonstrated that the oxidative stress effect was induced by HEX enantiomers in the earthworms, and the earthworm antioxidant defense system began to defend against the damage caused by excessive ROS. Similar results have been reported in a previous study by Zhang et al. (2012b), who reported that a certain dose of fomesafen induced oxidative stress in the earthworm. In their study, the CAT activity of the target compound treatment group also first decreased and then increased. In general, the HEX enantiomers affected the oxidation system of earthworms; in particular, *S*-(+)-HEX had a stronger inhibitory effect.

CYP450 is involved in the phase I metabolism of many xenobiotics and is widely used as a biomarker of pollutants (Lu et al., 2017). Triazole compounds inhibit cytochrome P-450-mediated oxidative demethylation, which is necessary for the synthesis of ergosterol and the conversion of kaurene to kaurenoic acid in the gibberellin biosynthesis pathway (Zhang et al., 2012a). In the present study, following the *S*-(+)-HEX treatments, the relative activity of CYP450 significantly decreased on days 3, 7, and 14 compared with that in the control and *R*-(−)-HEX groups ($p < 0.05$, Fig. 5C). However, the activity of CYP450 in both the *S*-(+)-HEX and *R*-(−)-HEX treatments returned to the control level on days 28 and 42, respectively. AChE is a key enzyme in biological nerve conduction, and changes in its activity are used as a biomarker in pesticide exposure studies (Wang et al., 2015). Compared with the control treatment, a significant inhibition effect on the activities of AChE was observed following *S*-(+)-HEX and *R*-(−)-HEX exposure throughout the exposure period ($p < 0.05$, Fig. 5D). Among them, the *S*-(+)-HEX treatment showed a significant inhibitory effect on the activities of AChE on days 3 and 7 compared with that seen in the *R*-(−)-HEX treatments ($p < 0.05$). The decreased CYP450 and AChE activities may be induced by pollutants exceeding the removal capacity of the detoxification system, leading to abnormal cell function. Moreover, the present results demonstrated that the nerve conduction and detoxification functions of the earthworms were significantly inhibited by the two tested compounds, meanwhile, the two enzymes might play an important role in the metabolism of HEX enantiomers in earthworms. Although AChE was not the target enzyme of the triazole fungicide, previous reports by Kolesárová et al. (2013) and Toni et al. (2011) have found that the AChE activities of cattle blood and *Cyprinus carpio* change after exposure to the triazole fungicide tebuconazole. Ergosterol biosynthesis-inhibiting fungicides, including HEX, can induce CYP450 forms responsible for activation of the OPs, which can lead to the inhibition of AChE activities (Kolesárová et al., 2013; Toni et al., 2011). Thus, previous reports and the present study indicated that biological enzymes were of great significance in protecting earthworms from oxidative damage induced by

environmental stresses. Notably, stronger induction effects of oxidative damage were observed in the case of *S*-(+)-HEX.

3.6. Enantioselective effects of HEX on biomacromolecules in earthworms

Most of the biological macromolecules can bind and react with ·OH⁻, such as lipids, proteins, and polysaccharides (Schieber et al., 2014). In addition, ·OH⁻ cannot be directly eliminated by the corresponding enzymes, and excess ·OH⁻ will cause oxidative damage to cells, such as the loss of enzyme activity and DNA damage, leading to apoptosis (Codreanu et al., 2015; Winterbourn et al., 2015). DNA may undergo DNA strand breaks, chain breaks, and base modification under oxidative stress (Lushchak et al., 2014).

8-OHdG is the ·OH⁻ adduct of dG in DNA, which is widely regarded as one of the most representative biomarkers that reflects DNA oxidative damage (Guo et al., 2016). As shown in Fig. 6A, no significant difference was observed in 8-OHdG on day 3 ($p > 0.05$). However, compared with that in the control treatments, a significant increase was observed on days 7 and 14 following *S*-(+)-HEX and *R*-(−)-HEX exposure ($p < 0.05$). Additionally, on days 28 and 42, no differences were observed in 8-OHdG content between the *R*-(−)-HEX treatment and control treatment ($p > 0.05$), whereas the *S*-(+)-HEX treatment induced a significantly enhanced 8-OHdG content ($p < 0.05$). ROS attack polysaturated fatty acids on biological cell membranes, leading to membrane lipid peroxidation. MDA, a product of lipid peroxidation, has become a typical indicator of the level of oxidative damage (Chen et al., 2011). As shown in Fig. 6B, significant increases in MDA content were observed in the *S*-(+)-HEX treatment on days 3, 28, and 42 ($p < 0.05$). The MDA content following *S*-(+)-HEX and *R*-(−)-HEX exposure was significantly increased on day 7 compared with that in the control treatment ($p < 0.05$). However, no significant difference was observed on day 14 ($p > 0.05$). Significant changes in the MDA and 8-OHdG contents showed that oxidative damage in the earthworms was caused by exposure to *S*-(+)-HEX and *R*-(−)-HEX. Additionally, the difference in the MDA and 8-OHdG contents induced by the two tested chemicals indicated that *S*-(+)-HEX and *R*-(−)-HEX had selective behaviors in combination with biomacromolecules. Research has shown that most biomacromolecules found in cells are chiral, and the enantiomers of chiral compounds have different combined effects with biomacromolecules because of their different spatial configurations, resulting in different toxic effects (Inaki et al., 2018). The present study demonstrated that *S*-(+)-HEX had a stronger interaction effect with biomacromolecules than that of *R*-(−)-HEX.

3.7. Differences in the transcriptomic profiles of the HEX enantiomers

The transcriptome analysis data were saved in the sequence read archive (SRA) of NCBI, with the BioProject ID of PRJNA664315. Transcriptome analysis is a powerful tool to study gene expression in earthworms after exposure to pollutants, and the results of the differentially expressed gene (DEG) analysis are shown in Fig. 7A. The number of DEGs was 9377 between the *R*-(−)-HEX-exposed treatment and control groups. Among them, 4695 genes were upregulated, and 4682 genes were downregulated. Between the control group and *S*-(+)-HEX treatment, the number of DEGs was 13,958. Among them, 4378 genes were upregulated, and 9580 genes were downregulated. Thus, enantioselective effects were observed on the transcriptomic profiles after *E. fetida* was exposed to HEX enantiomers. Moreover, the total number of DEGs in the *S*-(+)-HEX exposure treatment was higher than that in the *R*-(−)-HEX exposure treatment, indicating that *S*-(+)-HEX may induce stronger toxic effects in earthworms than *R*-(−)-HEX.

DEGs will influence certain biological functions in organisms, and the biological role of DEGs can be evaluated using KEGG category enrichment analysis (Chai et al., 2020). Twenty significantly enriched pathways are listed in Fig. 7B. Among these 20 pathways, steroid biosynthesis, arachidonic acid metabolism, and cell cycle pathways were most influenced by *S*-(+)-HEX, whereas no significantly enriched pathway was found in the *R*-(−)-HEX-exposed treatment.

For the steroid biosynthesis pathways, steroid biosynthesis includes progesterone and estradiol, among others, which are essential for maintaining the reproductive physiology of female animals (Xu et al., 2018). The steroid biosynthesis pathway was severely affected, indicating that the effect of target compounds on the earthworms was gender-specific. Shen et al. (2013) studied the enantioselective disappearance of HEX enantiomers in rats and found that this disappearance was gender-related, whereas enantioselective changes of CYP450 activities were found after HEX enantiomer exposure. These findings were consistent with ours (Shen et al., 2013). Moreover, CYP450 is an important regulatory factor of the steroid biosynthesis pathway (Liu et al., 2018a). Therefore, we speculated that the inhibitory effect of HEX enantiomers on earthworms was not only enantioselective but also gender specific. Notably, the steroid biosynthesis pathway is simultaneously regulated by arachidonic acid-mediated metabolism signals (Zosmer et al., 2002). For the arachidonic acid metabolism pathways, arachidonic acid is a polyunsaturated fatty acid released by the lipolysis of phospholipids, and the CYP450 pathway affects the synthesis of arachidonic acid (Chang et al.,

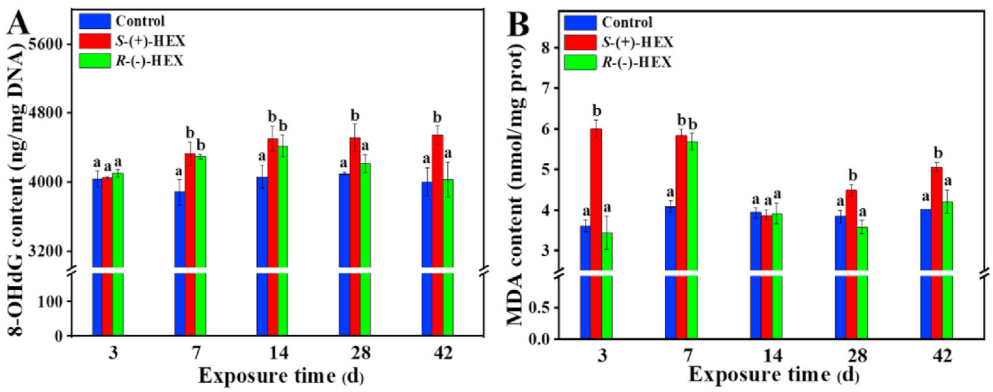

Fig. 6. Effects of *S*-(+)-HEX and *R*-(−)-HEX on 8-OHdG content (**A**) and MDA content (**B**) in earthworms.

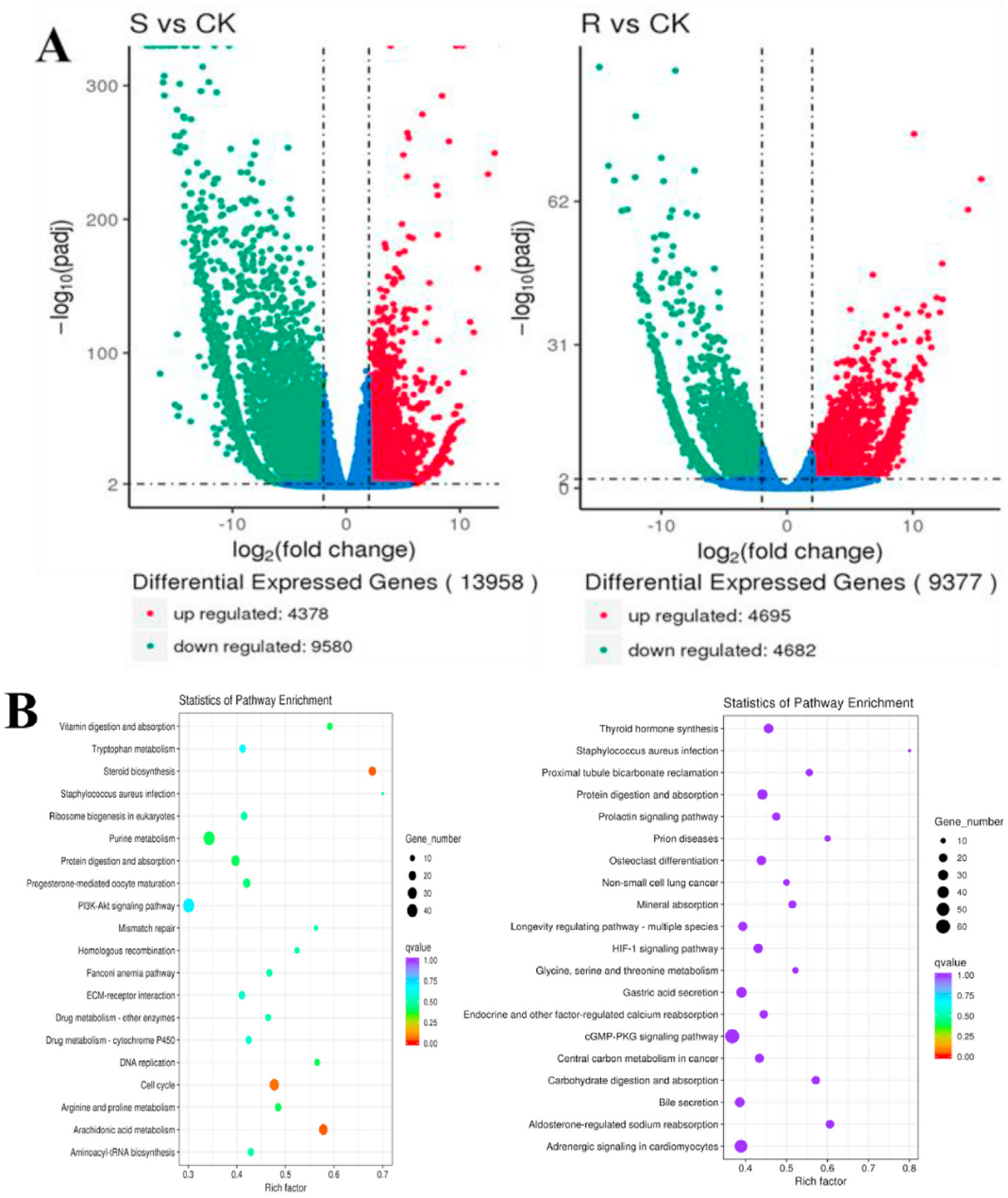

Fig. 7. Volcanic figure of DEGs after exposure to *S*-(+)-HEX and *R*-(−)-HEX compared with the control group (**A**) and function annotation of DEGs using KEGG database of *S*-(+)-HEX and *R*-(−)-HEX compared with the control group (**B**).

2014). The enrichment of arachidonic acid metabolism pathways indicated that the phospholipid metabolism capability in *E. fetida* was inhibited, disrupting the function of CYP450. In the present study, CYP450 activity was inhibited after exposure to *S*-(+)-HEX, which is consistent with the results of transcriptomic analysis. Moreover, ROS combine with polyunsaturated fatty acids to cause membrane lipid peroxidation, which may induce arachidonic acid, a source of polyunsaturated fatty acids, to be metabolized abnormally (Wong et al., 2015). Additionally, in the subchronic toxicity test, the content of MDA that is related to lipid metabolism increased at day 42 after exposure to *S*-(+)-HEX, which corroborates the enrichment result of arachidonic acid metabolism pathways. For the cell cycle pathway, the regulation of the cell cycle is a basic process in eukaryotes. Before entering mitosis, the cell determines that the DNA has completely replicated in the S phase, and the DNA is not damaged (Reinhardt et al., 2010; Yang et al., 2014). Therefore, the significantly enriched cell cycle pathways may suggest that the earthworm cellular DNA replication process was destroyed. Studies have shown that oxidative stress produced by ROS can induce DNA damage and stimulate neuronal cells to re-enter the cell cycle (Itsang Chiang et al., 2015). In the present study, 8-OHdG levels were abnormally elevated after exposure to *S*-(+)-HEX, which coincided with the enrichment of the cell cycle pathway. In the present study, ROS induction by the test chemical influenced steroid biosynthesis, the cell cycle, and arachidonic acid metabolism, leading to enantioselective oxidative damage, DNA damage, and other effects, which caused damage to functional molecules in the earthworm organisms, such as detoxifying enzymes and biological macromolecules.

In this study, the *S*-(+)-HEX degraded more slowly than *R*-

(−)-HEX in the artificial soil. However, the bioaccumulative effect was opposite to that of soil degradation. In the earthworms, *S*-(+)-HEX accumulated faster than *R*-(−)-HEX. The differences in degradation and bioaccumulation may be due to the difference in steric configuration between *S*-(+)-HEX and *R*-(−)-HEX. The configuration of *R*-(−)-HEX has a stronger combining capacity with environmental media or biomacromolecules in microorganisms. Accordingly, *S*-(+)-HEX has a higher affinity with the biomacromolecules in earthworms, ultimately resulting in excessive accumulation. For the earthworms, both *S*-(+)-HEX and *R*-(−)-HEX were exogenous pollutants and their accumulation induced stress responses in cells, such as increased ROS content. In order to prevent ROS from damaging the cell function, the antioxidant defense system began to clear the excess ROS by regulating the activities of SOD and CAT. With an increase in exposure time, an increasing amount of *S*-(+)-HEX and *R*-(−)-HEX accumulated in the earthworms and finally caused damage to biomacromolecules, leading to various damage effects, such as lipid peroxidation and DNA damage. Through transcriptome sequencing, differentially expressed genes and significantly enriched pathways were discovered. The transcriptome sequencing results showed that steroid biosynthesis, arachidonic acid metabolism, and cell cycle pathways were most influenced by *S*-(+)-HEX. These pathways were related to the function of phospholipid metabolism, DNA replication, etc., which were consistent with the changes in the activities of CYP450 and the contents of MDA and 8-OHdG. The present study demonstrated that *S*-(+)-HEX may pose a higher environmental risk than *R*-(−)-HEX, and the risk assessment of HEX should be performed at the enantiomeric level.

4. Conclusion

In the present study, the toxicity and bioaccumulation of HEX enantiomers in earthworms were investigated. HEX enantiomers exhibited significantly enantioselective degradation in artificial soils, with a preferential degradation of *R*-(−)-HEX. No significant differences in bioaccumulation were found in earthworms during the entire exposure period; however, the acute toxicity of *S*-(+)-HEX was 2.59 times higher than that of *R*-(−)-HEX. *S*-(+)-HEX and *R*-(−)-HEX induced oxidative stress and destroyed the function of biomacromolecules such as lipids and proteins. Moreover, *S*-(+)-HEX showed a stronger interaction effect with biomacromolecules than *R*-(−)-HEX. *S*-(+)-HEX displayed a stronger influence on steroid biosynthesis, cell cycle, and arachidonic acid metabolism pathways, which may be the primary reason for the enantioselective behavior of HEX enantiomers. Thus, the risk assessment of HEX should be performed at the enantiomeric level, and *S*-(+)-HEX may pose a high environmental risk.

Declaration of competing interest

The authors declare that they have no known competing financial interests or personal relationships that could have appeared to influence the work reported in this paper.

Acknowledgments

The present study was supported by grants from the National Natural Science Foundation of China, China (No. 42007376) and the Shandong Provincial Natural Science Foundation, China (No. ZR2017BD028028ZR).

Appendix A. Supplementary data

Supplementary data to this article can be found online at https://doi.org/10.1016/j.envpol.2020.116269.

References

Bates, L.S., Waldren, R.P., Teare, I.D., 1973. Rapid determination of free proline for water-stress studies. Plant Soil 39, 205–207.
Chai, L., Yang, Y., Yang, H., Zhao, Y., Wang, H., 2020. Transcriptome analysis of genes expressed in the earthworm *Eisenia fetida* in response to cadmium exposure. Chemosphere 240, 124902.
Chang, Q., Berdyshev, E., Cao, D., Bogaard, J.D., White, J.J., Chen, S., Grassi, M.A., 2014. Cytochrome P450 2C epoxygenases mediate photochemical stress-induced death of photoreceptors. J. Biol. Chem. 289 (12), 8337–8352.
Chen, C., Zhou, Q., Liu, S., Xiu, Z., 2011. Acute toxicity, biochemical and gene expression responses of the earthworm *Eisenia fetida* exposed to polycyclic musks. Chemosphere 83 (8), 1147–1154.
Chen, J.H., Wang, H.L., Guo, B.Y., Li, J.Z., 2013. LC-MS/MS method for simultaneous determination of myclobutanil, hexaconazole, diniconazole, epoxiconazole and tetraconazole enantiomers in soil and earthworms. Int. J. Environ. Anal. Chem. 94 (8), 791–800.
Chen, C., Yang, Z., Kong, F.X., Zhang, M., Yu, Y., Shi, X.L., 2016. Growth, physiochemical and antioxidant responses of overwintering benthic cyanobacteria to hydrogen peroxide. Environ. Pollut. 219, 649–655.
Codreanu, S.G., Liebler, D.C., 2015. Novel approaches to identify protein adducts produced by lipid peroxidation. Free Radic. Res. 49, 881–888.
Cui, N., Xu, H., Yao, S., He, Y., Zhang, H., Yu, Y., 2018. Chiral triazole fungicide tebuconazole: enantioselective bioaccumulation, bioactivity, acute toxicity, and dissipation in soils. Environ. Sci. Pollut. Res. 25 (25), 25468–25475.
Dubey, P., Mishra, A.K., Singh, A.K., 2015. Comparative analyses of genotoxicity, oxidative stress and antioxidative defence system under exposure of methyl parathion and hexaconazole in barley (*Hordeum vulgare* L.). Environ. Sci. Pollut. Res. 22 (24), 19848–19859.
Feng, M., Yin, H., Peng, H., Liu, Z., Lu, G., Dang, Z., 2017. Hexavalent chromium induced oxidative stress and apoptosis in *Pycnoporus sanguineus*. Environ. Pollut. 228, 128–139.
Gámiz, B., Facenda, G., Celis, R., 2016. Evidence for the effect of sorption enantioselectivity on the availability of chiral pesticide enantiomers in soil. Environ. Pollut. 213, 966–973.
Gao, M., Song, W., Zhang, J., Guo, J., 2013. Effect on enzymes and histopathology in earthworm (*Eisenia foetida*) induced by triazole fungicides. Environ. Toxicol. Pharmacol. 35 (3), 427–433.
Gao, J., Wang, F., Jiang, W., Miao, J., Wang, P., Zhou, Z., Liu, D., 2020. A full evaluation of chiral phenylpyrazole pesticide flufiprole and the metabolites to non-target organism in paddy field. Environ. Pollut. 264, 114808.
Garrison, A.W., 2011. An introduction to pesticide chirality and the consequences of stereoselectivity. ACS Symp. Ser. 1–7.
Gill, S.S., Tuteja, N., 2010. Reactive oxygen species and antioxidant machinery in abiotic stress tolerance in crop plants. Plant Physiol. Biochem. (Paris) 48, 909–930.
Guo, Z., Liu, X., Liu, Y., Wu, G., Lu, X., 2016. Constructing a novel 8-hydroxy-2'-deoxyguanosine electrochemical sensor and application in evaluating the oxidative damages of DNA and guanine. Biosens. Bioelectron. 86, 671–676.
Han, J., Jiang, J., Su, H., Sun, M., Wang, P., Liu, D., Zhou, Z., 2013. Bioactivity, toxicity and dissipation of hexaconazole enantiomers. Chemosphere 93 (10), 2523–2527.
Inaki, M., Sasamura, T., Matsuno, K., 2018. Cell chirality drives left-right asymmetric morphogenesis. Front. Cell Dev. Biol. 6, 34.
Itsang Chiang, W., Wang, S., Liu, Hsinchung, T Yang, S., Tang, N.Y., Chung, J.G., 2015. Curcumin alters gene expression-associated DNA damage, cell cycle, cell survival and cell migration and invasion in NCI-H460 human lung cancer cells in vitro. Oncol. Rep. 34 (4), 1853–1874.
Ju, C., Xu, J., Wu, X., Dong, F., Liu, X., Tian, C., Zheng, Y., 2017. Effects of hexaconazole application on soil microbes community and nitrogen transformations in paddy soils. Sci. Total Environ. 609, 655–663.
Kolesárová, V., Šinko, G., Siviková, K., Dianovský, J., 2013. In vitro inhibition of blood cholinesterase activities from cattle by triazole fungicides. Caryologia 66 (4), 346–350.
Konwick, B.J., Garrison, A.W., Black, M.C., Avants, J.K., Fisk, A.T., 2006. Bioaccumulation, biotransformation, and metabolite formation of fipronil and chiral legacy pesticides in rainbow trout. Environ. Sci. Technol. 40, 2930–2936.
Liang, H., Li, L., Li, W., Wu, Y., Liu, F., 2011. The decline and residues of hexaconazole in tomato and soil. Environ. Monit. Assess. 184, 1573–1579.
Li, Y., Dong, F., Liu, X., Xu, J., Chen, X., Han, Y., Zheng, Y., 2013. Studies of enantiomeric degradation of the triazole fungicide hexaconazole in tomato, cucumber, and field soil by chiral liquid chromatography-tandem mass spectrometry. Chirality 25 (3), 160–169.
Liu, J., Zhang, X., Sun, Y., Lin, W., 2010. Antioxidative capacity and enzyme activity in *Haematococcus pluvialis* cells exposed to superoxide free radicals. Chin. J. Oceanol. Limnol. 28 (1), 1–9.
Liu, T.T., Diao, J.L., Di, S.S., Zhou, Z., 2014. Stereoselective bioaccumulation and metabolite formation of triadimefon in *Tubifex tubifex*. Environ. Sci. Technol. 48, 6687–6693.
Liu, T., Zhu, L.S., Wang, J.H., Wang, J., Tan, M.Y., 2016. Phytotoxicity of imidazolium-based ILs with different anions in soil on *Vicia faba* seedlings and the influence of anions on toxicity. Chemosphere 145, 269–276.

Liu, J., Li, X., Yao, Y., Li, Q., Pan, Z., Li, Q., 2018a. miR-1275 controls granulosa cell apoptosis and estradiol synthesis by impairing LRH-1/CYP19A1 axis. Biochim. Biophys. Acta, Gene Regul. Mech. 1861 (3), 246–257.
Liu, T., Chen, D., Li, Y., Wang, X., Wang, F., 2018b. Enantioselective bioaccumulation and toxicity of the neonicotinoid insecticide dinotefuran in earthworms (*Eisenia fetida*). J. Agric. Food Chem. 66 (17), 4531–4540.
Lu, X., Li, Y., Thunders, M., Cavanagh, J., Matthew, C., Wang, X., Qiu, J., 2017. Differential protein expression and localization of CYP450 enzymes in three species of earthworm; is this a reflection of environmental adaptation? Chemosphere 171, 485–490.
Lushchak, V.I., 2014. Free radicals, reactive oxygen species, oxidative stress and its classification. Chem. Biol. Interact. 224, 164–175.
Ma, J., Cheng, C., Du, Z., Li, B., Wang, J., Wang, J., Zhu, L., 2019. Toxicological effects of pyraclostrobin on the antioxidant defense system and DNA damage in earthworms (*Eisenia fetida*). Ecol. Indicat. 101, 111–116.
Ma, Y., Gan, J., Liu, W., 2011. Chiral pesticides and environmental safety. ACS Symp. Ser. 97–106.
Maznah, Z., Halimah, M., Ismail, S., Idris, A.S., 2015. Dissipation of the fungicide hexaconazole in oil palm plantation. Environ. Sci. Pollut. Res. 22 (24), 19648–19657.
OECD, 1984. Test 207: Earthworm, Acute Toxicity Tests, pp. 1–9.
Reinhardt, H.C., Hasskamp, P., Schmedding, I., Morandell, S., van Vugt, M.A.T.M., Wang, X., Yaffe, M.B., 2010. DNA damage activates a spatially distinct late cytoplasmic cell-cycle checkpoint network controlled by MK2-mediated RNA stabilization. Mol. Cell. 40 (1), 34–49.
Schieber, M., Chandel, N.S., 2014. ROS function in redox signaling and oxidative stress. Curr. Biol. 24, 453–462.
Shahid, M., Khan, M.S., 2018. Fungicide tolerant *Bradyrhizobium japonicum* mitigate toxicity and enhance greengram production under hexaconazole stress. J. Environ. Sci. 31, 92–108.
Shen, Z., Liu, D., Wang, P., Zhang, P., Wang, X., Zhou, Z., 2013. Gender-related in vitro metabolism of hexaconazole and its enantiomers in rats. Chirality 25 (12), 852–857.
Tian, F., Liu, X., Wu, Y., Xu, J., Dong, F., Wu, X., Zheng, Y., 2016. Simultaneous determination of penflufen and one metabolite in vegetables and cereals using a modified quick, easy, cheap, effective, rugged, and safe method and liquid chromatography coupled to tandem mass spectrometry. Food Chem. 213, 410–416.
Toni, C., Loro, V.L., Santi, A., de Menezes, C.C., Cattaneo, R., Clasen, B.E., Zanella, R., 2011. Exposure to tebuconazole in rice field and laboratory conditions induces oxidative stress in carp (*Cyprinus carpio*). Comp. Biochem. Physiol. 153 (1), 128–132.
Wang, H., Zhang, X., Wang, L., Zhu, B., Guo, W., Liu, W., Wang, J., 2020. Biochemical responses and DNA damage induced by herbicide QYR301 in earthworm (*Eisenia fetida*). Chemosphere 244, 125512.
Wang, X., Zhang, H., Xu, H., Wang, X., Wu, C., Yang, H., Wang, Q., 2012. Enantioselective residue dissipation of hexaconazole in cucumber (*Cucumis sativus* L.), head cabbage (*Brassica oleracea* L. var. *caulorapa* DC.), and soils. J. Agric. Food Chem. 60 (9), 2212–2218.
Wang, Y., Liu, C., Gao, J., Wang, C., Cui, L., Li, A., 2014. Dissipation behavior of hexaconazole and kresoxim-methyl residues in ginseng and soil under field conditions. Environ. Monit. Assess. 187 (1).
Wang, K., Mu, X., Qi, S., Chai, T., Pang, S., Yang, Y., Jiang, J., 2015. Toxicity of a neonicotinoid insecticide, guadipyr, in earthworm (*Eisenia fetida*). Ecotoxicol. Environ. Saf. 114, 17–22.
Winterbourn, C.C., 2015. Are free radicals involved in thiol-based redox signaling? Free Radic. Biol. Med. 80, 164–170.
Wong, D., Hu, X., Tao, N., Wang, X., Wang, M., 2015. Effect and mechanism of pyridoxamine on the lipid peroxidation and stability of polyunsaturated fatty acids in beef patties. J. Sci. Food Agric. 96 (10), 3418–3423.
Xu, P., Liu, D.H., Diao, J.L., Lu, D.H., Zhou, Z.Q., 2009. Enantioselective acute toxicity and bioaccumulation of benalaxyl in earthworm (*Eisenia fedtia*). J. Agric. Food Chem. 57, 8545–8549.
Xu, D., He, H., Jiang, X., Hua, R., Chen, H., Yang, L., Li, Q., 2018. SIRT2 plays a novel role on progesterone, estradiol and testosterone synthesis via PPARs/LXRα pathways in bovine ovarian granular cells. J. Steroid Biochem. Mol. Biol. 185, 27–38.
Yang, Q., He, X., Li, X., Xu, W., Luo, Y., Yang, X., Huang, K., 2014. DNA damage and S phase arrest induced by Ochratoxin A in human embryonic kidney cells (HEK 293). Mutat. Res. Fund Mol. Mech. Mutagen 765, 22–31.
Yu, D., Li, J., Zhang, Y., Wang, H., Guo, B., Zheng, L., 2012. Enantioselective bioaccumulation of tebuconazole in earthworm *Eisenia fetida*. J. Environ. Res. 24 (12), 2198–2204.
Yu, L., Chen, M., Liu, Y., Gui, W., Zhu, G., 2013. Thyroid endocrine disruption in zebrafish larvae following exposure to hexaconazole and tebuconazole. Aquat. Toxicol. 138–139, 35–42.
Zhang, P., Dang, Z., Shen, Z., Zhu, W., Xu, X., Liu, D., Zhou, Z., 2012a. Enantioselective degradation of hexaconazole in rat hepatic microsomes in vitro. Chirality 24 (4), 283–288.
Zhang, Q., Zhu, L., Wang, J., Xie, H., Wang, J., Han, Y., Yang, J., 2012b. Oxidative stress and lipid peroxidation in the earthworm *Eisenia fetida* induced by low doses of fomesafen. Environ. Sci. Pollut. Res. 20 (1), 201–208.
Zhang, S., Ding, J., Razanajatovo, R.M., Jiang, H., Zou, H., Zhu, W., 2019. Interactive effects of polystyrene microplastics and roxithromycin on bioaccumulation and biochemical status in the freshwater fish red tilapia (*oreochromis niloticus*). Sci. Total Environ. 648, 1431–1439.
Zhang, R., Zhou, Z., 2019. Effects of the chiral fungicides metalaxyl and metalaxyl-M on the earthworm *Eisenia fetida* as determined by 1H-NMR-based untargeted metabolomics. Molecules 24 (7), 1293.
Zhang, C., Zhou, T., Du, Z., Albert, J., Zhu, L., Wang, J., Wang, J., Li, B., 2020. Applying fungicide on earthworms: biochemical effects of *Eisenia fetida* exposed to fluoxastrobin in three natural soils. Environ. Pollut. 258, 113666.
Zhou, B.H., Zhao, J., Liu, J., Zhang, J.L., Li, J., Wang, H.W., 2015. Fluoride-induced oxidative stress is involved in the morphological damage and dysfunction of liver in female mice. Chemosphere 139, 504–511.
Zosmer, A., Elder, M., Sullivan, M.H., 2002. The production of progesterone and 5,6-epoxyeicosatrienoic acid by human granulosa cells. J. Steroid Biochem. Mol. Biol. 81 (4–5), 369–376.